

SUPER-LATTICE STRUCTURE PHOTONIC CRYSTAL FIBER

D. Chen [†], M.-L. V. Tse, and H. Y. Tam

Photonics Research Centre, Department of Electrical Engineering
The Hong Kong Polytechnic University
Hung Hom, Kowloon, Hong Kong SAR, China

Abstract—We propose a kind of novel photonic crystal fibers (PCFs) based on a super-lattice structure. Uniform air holes are used to form the basic cell structure. Using the uniform air holes in the PCF has the advantage of minimizing the structural distortion during fabrication while forming a complex-structure cross section. We propose an effective-circular-hole PCF with the similar properties of the conventional circular-hole PCF to address the concept of the super-lattice structure PCF. An effective-elliptical-hole PCF based on a super-lattice structure is proposed and investigated, which has similar birefringent and confinement loss characteristics as the previously reported elliptical-hole PCF. Other PCFs based on super-lattice structures such as the effective-triangular-hole PCF and effective-rectangular-hole PCF can also be achieved by using the design method proposed in this paper.

1. INTRODUCTION

Photonic crystal fibers (PCFs) [1–3] which have the flexibility for the cross section design have attracted considerable attention over the past decade because of both their unique properties in birefringence [4], dispersion [5], nonlinearity [6], effective mode area [7] and their excellent performances in the applications of fiber sensors [8, 9], fiber lasers [10–12] and nonlinear optics [13, 14]. Many studies focus on the performance of PCFs as functional components or devices instead of a transmission medium. To achieve a specific function of a PCF, the cross section of the PCF can be very complex. For example, many

Corresponding author: D. Chen (daru@coer.zju.edu.cn).

[†] Also with Institute of Information Optics, Zhejiang Normal University, Jinhua 321004, China.

designs have been proposed to achieve a single-polarization single-mode (SPSM) PCF [15–18] and dispersion-flattened (DF) PCF [19, 20]. Early PCF designs were proposed to achieve SPSM and DF PCFs by employing circular air holes of different diameters. More recently, novel SPSM PCFs employing elliptical air holes of different sizes [17], or using both elliptical air holes and circular air holes [18] in the cross section are proposed to achieve a larger SPSM operation band. Moreover, PCFs with complex cross section were also designed to achieve high birefringence [21–24]. However, it is very challenging for the fabrication of those kinds of PCFs, since both the exact air hole size and shape are very important for those PCFs with complex cross section. In order to compensate different surface tensions of the air holes with different diameters, complex pressure control is needed to accurately produce the air hole of different sizes during fabrication. Air holes will always tend to become circular during the fabrication because of the unavoidable surface tension. It is almost impossible to accurately fabricate PCFs with different kinds of complex noncircular air holes (e.g., the SPSM PCF reported in [17, 18]) using the current fabrication techniques available.

In this paper, we propose a kind of novel PCFs based on a super-lattice structure, which will minimize the structural distortion during fabrication, at the same time, achieving the unique optical property of the PCFs with complex structures. Small circular air holes are used to build the basic cell (structure unit) in the cross section of the PCFs, which will potentially overcome the fabrication challenge because of the uniform hole size. The small circular air holes can be combined to build a complex air-filling area, which represent an effectively large air hole of complex shape. We investigate in detail two examples of the proposed super-lattice structures based PCFs, one PCF design with effective-circular-holes and the other with effective-elliptical-holes. The proposed effective-elliptical-hole PCF is with high birefringence (even up to 0.01) and lower confinement loss than the conventional elliptical-hole PCF.

2. EFFECTIVE-CIRCULAR-HOLE PCF BASED ON A SUPER-LATTICE STRUCTURE

In this section, we will first introduce the concept of a super-lattice structure PCF. It is worthwhile to note that Wang et al. has proposed a supercell lattice method for PCF modeling [25] which is quite different from the concept for super-lattice structure PCF (structure design method) in this paper.

Figure 1(a) shows the cross sections of an effective-circular-

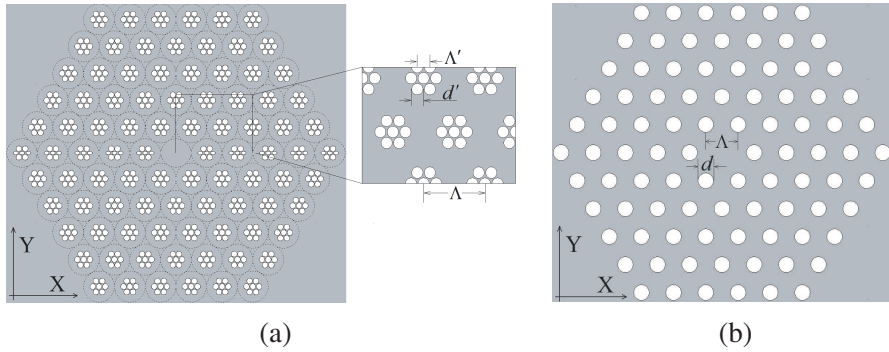


Figure 1. Cross sections of (a) an effective-circular-hole PCF based on a super-lattice structure and (b) a conventional circular-hole PCF. (Dotted circles indicate potential cane elements).

hole PCF based on a super-lattice structure, and Fig. 1(b) shows a conventional circular-hole PCF. For the effective-circular-hole PCF, 7 small air holes form a basic cell structure. The cell structure works as a large effective-circular air hole that is found in a conventional PCF. The 7 air holes are arranged in a structure of hexagonal lattice with pitch, Λ' , which ensures stability and flexibility when making the fiber preform. 5 rings of basic cells (large effective-circular air holes) are employed in the fiber cladding of the PCF with a cell-to-cell spacing lattice constant Λ (i.e., the pitch of the large effective-circular air holes where each is formed by 7 small air holes).

We employ a full-vector finite-element method (FEM) [26] and anisotropic perfectly matched layers to investigate the guided modes of the proposed PCF. The confinement loss can be deduced from the imaginary part of the effective modal index. In what follows, the refractive indexes of fused silica and air are assumed to be 1.45 and 1, respectively. Calculated results are expressed in terms of the normalized frequency $\nu = \Lambda/\lambda$, where λ is the operation wavelength in free space. The effective-circular-hole PCF with the structure shown in Fig. 1(a) has the parameters of $\Lambda = 2.2 \mu\text{m}$, $\Lambda' = 0.5 \mu\text{m}$, and $d' = 0.4 \mu\text{m}$. For comparison, the circular-hole PCF with the structure shown in Fig. 1(b) has the same lattice constant (Λ) and air-filling fraction as the effective-circular-hole PCF (air-filling fraction = 20.99%, $d/\Lambda = 0.481$).

Figure 2 shows the effective index of the x -polarized (black solid circles for effective-circular-hole PCF and black solid rectangles for circular-hole PCF) and y -polarized (red hollow circles for effective-circular-hole PCF and green hollow rectangles for circular-hole PCF)

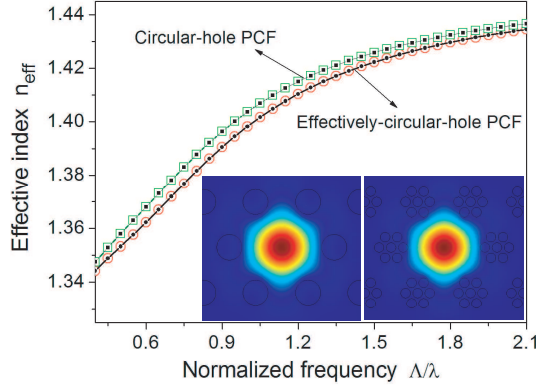


Figure 2. Effective index of the x -polarized and y -polarized fundamental modes as a function of normalized frequency for the effective-circular-hole PCF and the conventional circular-hole PCF. Inset shows the power flow of the y -polarized fundamental modes at normalized frequency $\nu = 1$ for the conventional circular-hole PCF (left inset) and the effective-circular-hole PCF (right inset).

fundamental modes as a function of normalized frequency. Inset shows the power flow of the y -polarized fundamental mode at $\nu = 1$ for the conventional circular-hole PCF (left inset) and the effective-circular-hole PCF (right inset). Note that the effective index curves of the x - and y -polarized fundamental modes for both the effective-circular-hole PCF and circular-hole PCF show that the two kinds of PCFs exhibit small birefringence. This can be understood due to the fact that the 7 small air holes with a hexagonal lattice structure can be an effective-circular hole. Both Λ' and d' can affect the effective index of the effective-circular-hole PCF.

Figure 3(a) shows the effective index (black hollow circles for effective-circular-hole PCF and black hollow rectangles for circular-hole PCF) and confinement loss (red solid circles for effective-circular-hole PCF and red solid rectangles for circular-hole PCF) of the y -polarized fundamental mode for different diameters of the small air holes (d') with $\Lambda = 2.2 \mu\text{m}$ and $\Lambda' = 0.5 \mu\text{m}$, and the parameters of the circular-hole PCF have the same lattice constant (Λ) and equivalent air-filling fraction. For both kinds of PCFs, as the diameter of the small air hole (or corresponding air-filling fraction) increases, both the effective index and confinement loss decrease. Moreover, it is found that the confinement loss of the circular-hole PCF is larger than that of the effective-circular-hole PCF. Fig. 3(b) shows the effective index

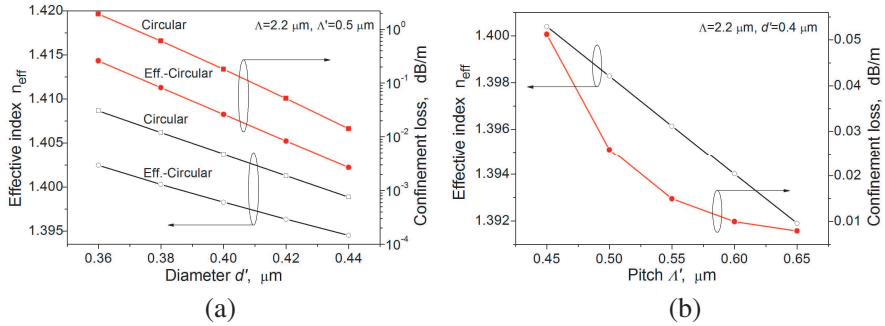


Figure 3. (a) Effective index (black hollow circles for effective-circular-hole PCF and black hollow rectangles for circular-hole PCF) and confinement loss (red solid circles for effective-circular-hole PCF and red solid rectangles for circular-hole PCF) of the y -polarized fundamental mode for different diameters of the small air holes (or corresponding air-filling fraction). (b) Effective index (black hollow circles) and confinement loss (red hollow circles) of the y -polarized fundamental mode of the effective-circular-hole PCF for different pitches of the small air holes.

(black hollow circles) and confinement loss (red hollow circles) of the y -polarized fundamental mode for different pitches of the small air holes with $\Lambda = 2.2 \mu\text{m}$ and $d' = 0.4 \mu\text{m}$. As the pitch of the small air hole (Λ') increases, both the effective index and the confinement loss of the PCF decrease. These simulation results show that with the same air-filling fraction in the fiber cladding, the distribution of the small air holes will affect the effective index and confinement loss of the effective-circular-hole PCF.

3. EFFECTIVE-ELLIPTICAL-HOLE PCF BASED ON A SUPER-LATTICE STRUCTURE

The above section has shown that an effective-circular-hole PCF based on a super-lattice structure can achieve similar properties of the conventional circular-hole PCF. In this section we will show that the PCF based on a super-lattice structure can also achieve high birefringence just like the elliptical-hole PCF. Fig. 4(a) shows the cross sections of an effective-elliptical-hole PCF based on a super-lattice structure, and Fig. 4(b) shows a conventional elliptical-hole PCF. For the effective-elliptical-hole PCF, 9 small air holes form a basic cell structure with a diamond-shaped area which plays a role of an effective-elliptical air hole. Note that the overall structure can be arranged into

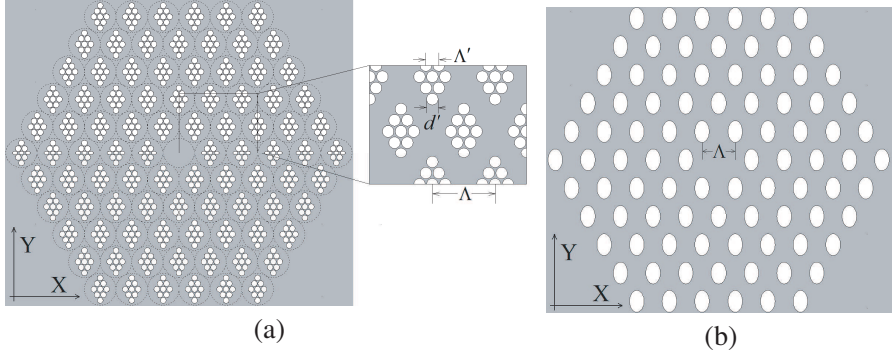


Figure 4. Cross sections of (a) an effective-elliptical-hole PCF based on a super-lattice structure and (b) a conventional elliptical-hole PCF. (Dotted circles indicate potential cane elements).

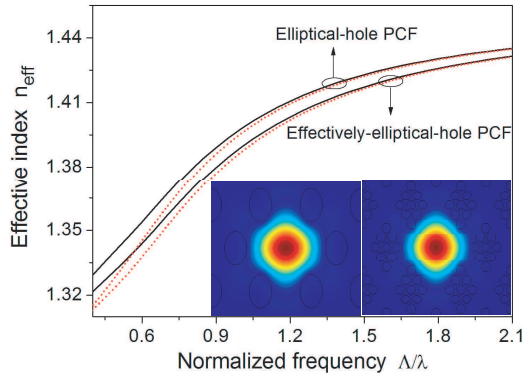


Figure 5. Effective index of the x -polarized (red dotted curves) and y -polarized (black solid curves) fundamental modes as a function of normalized frequency for the effective-elliptical-hole PCF and the conventional elliptical-hole PCF. Inset shows the power flow of the y -polarized fundamental mode de at $\nu = 1$ for the conventional elliptical-hole PCF (left inset) and the effective-elliptical-hole PCF (right inset).

a preform using the secondary stacking of canes method mentioned in Section 2.

Figure 5 shows the effective index of the x -polarized (red dotted curves) and y -polarized (black solid curves) fundamental modes as a function of normalized frequency for the effective-elliptical-hole PCF (with the parameters of $\Lambda = 2.2 \mu\text{m}$, $\Lambda' = 0.5 \mu\text{m}$, and $d' = 0.4 \mu\text{m}$) and the conventional elliptical-hole PCF with the same lattice constant

(Λ) and air-filling fraction (26.98%) as the effective-elliptical-hole PCF. The ellipticity of the elliptical air hole in the elliptical-hole PCF is set to be 1.5. Inset shows the power flow of the y -polarized fundamental mode at $\nu = 1$ for the conventional elliptical-hole PCF (left inset) and effective-elliptical-hole PCF (right inset). Evidently, the y -polarized modes have a higher effective index than the x -polarized ones for both kinds of PCFs, which indicates that they have high birefringence (in particular at the low normalized frequency). Note that the birefringence is defined as $\Delta n = n_y - n_x$ in this paper, where n_i ($i = x, y$) are the effective indexes (modal indexes).

Figure 6 shows both the birefringence property and confinement property of the effective-elliptical-hole PCF (black curves) and the

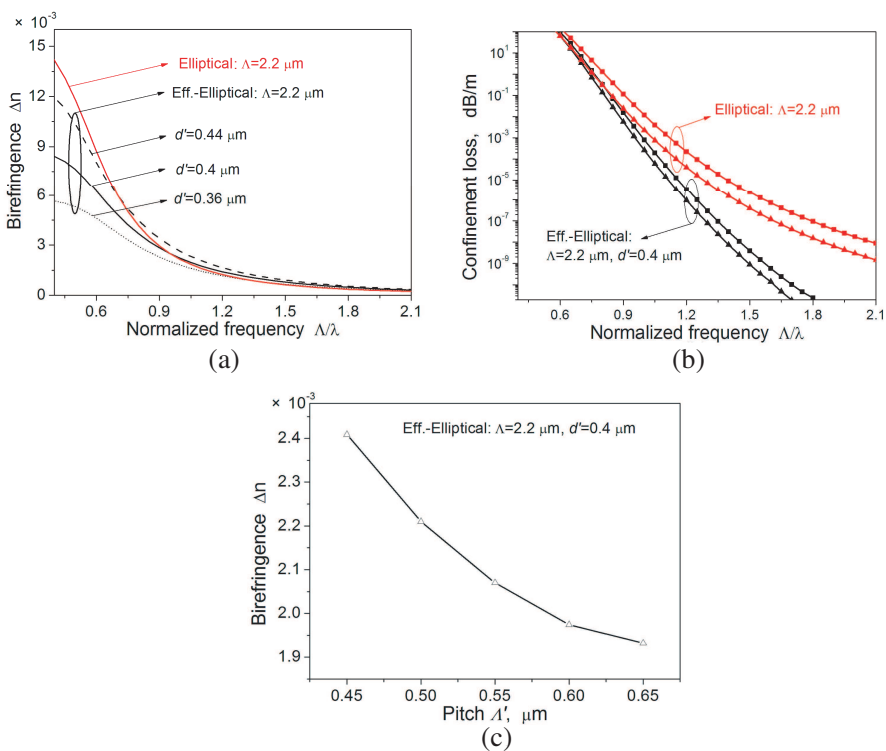


Figure 6. (a) Birefringence property of the effective-elliptical-hole PCF (black curves) and the elliptical-hole PCF (red curves). (b) Confinement property of the effective-elliptical-hole PCF (black curves) and the elliptical-hole PCF (red curves). (c) Birefringence of the effective-elliptical-hole PCF for different pitch of the small air holes.

elliptical-hole PCF (red curves). The previously reported elliptical-hole PCFs [21, 22] have been well investigated. The birefringence property (red solid curve) and confinement property of y -polarized (red curve with rectangles) and x -polarized (red curve with triangles) fundamental modes of the elliptical-hole PCF with a structure shown in Fig. 4(b) are shown in Figs. 6(a) and (b). High birefringence (up to the order of 10^{-2}) which is mainly introduced by the asymmetry of the fiber cladding can be achieved at the low normalized frequency (the power distributed in the fiber cladding and the confinement loss is relatively high). The proposed effective-elliptical-hole PCF with a structure shown in Fig. 4(a) has similar birefringence property (shown as black solid curve in Fig. 6(a)) and confinement property of the y -polarized (shown as black curve with rectangles in Fig. 6(b)) and x -polarized (shown as black curve with triangles in Fig. 6(b)) fundamental modes. It is observed that the birefringence curves of the two kinds of PCFs intersect at $\nu = 0.95$, shown in Fig. 6(a). The birefringence of the PCF is due to the effects of the asymmetry of both the fiber core and fiber cladding [17]. The proposed effective-elliptical-hole PCF has a core of higher asymmetry (due to the diamond shape of air hole area) compared with the elliptical-hole PCF, which results in higher birefringence for the effective-elliptical-hole PCF at the high normalized frequency (larger than 1). At the low normalized frequency, the birefringence is predominantly due to the effect of the asymmetry of the fiber cladding, and the elliptical-hole PCF has higher birefringence. In addition, the simulation results also show that the birefringence increases when the diameter of the small air hole increases

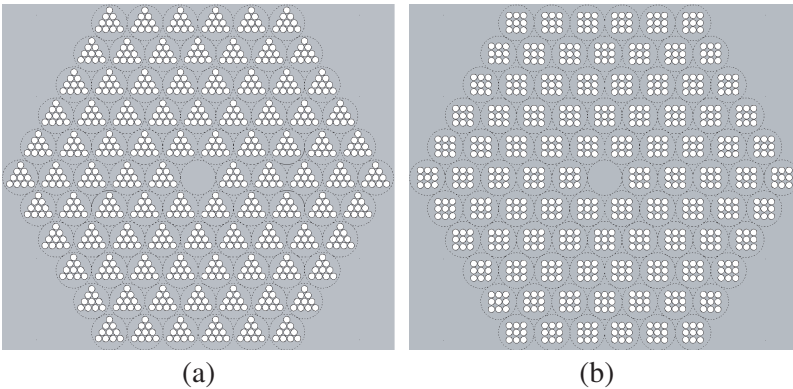


Figure 7. Cross sections of (a) an effective-triangular-hole PCF and (b) an effective-rectangular-hole PCF based on super-lattice structures.

for the effective-elliptical-hole PCF. The dashed and dotted curves show the birefringence of effective-elliptical-hole PCF with small air hole diameters of $d' = 0.36 \mu\text{m}$ and $d' = 0.44 \mu\text{m}$, respectively. Fig. 6(c) shows the relationship between the birefringence and the hole pitch of the small air holes (Λ') for the effective-elliptical-hole PCF with the parameters of $\Lambda = 2.2 \mu\text{m}$ and $d' = 0.4 \mu\text{m}$ when the normalized frequency is $\nu = 1$, which indicates that the proposed PCFs provides an additional parameter for highly birefringent PCF design.

4. DISCUSSION AND CONCLUSION

In general, the proposed super-lattice structure PCFs in this paper are with large potential benefits discussed as follows. Firstly, small air holes can be used to form the basic cell structure with effective index under flexible control, which has also been partially mentioned in our previous work [22]. It is shown with the example of the effective-circular-hole PCF in this paper. A basic cell formed by 7 small holes can be viewed as an effective circular hole, and the properties (effective index or dispersion) of the PCF are dependent on the parameters of the small holes. This concept can be extended to apply to complex dispersion-flattened PCF structures [20], in which, different circular hole sizes can be replaced with different numbers of small circular holes in the cell (cane) elements. Secondly, small circular holes can form a basic cell of an effective noncircular hole shape. With basic cell of diamond-shaped air area formed by 9 small holes, the proposed effective-elliptical-hole PCF in this paper has similar effective index and birefringence property to the elliptical-hole PCF. Besides the effective-elliptical-hole PCF, SPSM PCFs with a more complex cross section such as the ones recently reported in [18] with both circular and elliptical air holes in the cross section can also be replaced with a PCF based on super-lattice structure. Similarly it works for triangular and square/rectangular [27] hole designs shown in Fig. 7. Thirdly, the design of super-lattice structure PCFs with small and uniform air holes can reduce complications during fiber fabrication. It is difficult to fabricate PCFs with complex noncircular air holes because of the unavoidable surface tension. The super-lattice structure PCFs will potentially overcome the fabrication challenge because of the uniform hole size.

For the design of a super-lattice structure PCF specific property, optimized basic cell of the PCF should be achieved by optimizing parameters such as the number, size and pitch of the small air holes. Increasing the number of smaller holes can help to achieve increasingly complex air-filling area and index, which may be good to achieving

very specific property of the PCF. However, fabrication limit to make the smaller air hole open should be considered.

In conclusion, we have proposed a kind of novel PCFs based on a super-lattice structure. Both an effective-circular-hole PCF and an effective-elliptical-hole PCF based on a super-lattice structure have been investigated. Simulation results show that the PCFs based on the super-lattice structure can achieve the optical properties as the previously reported PCFs. Some of which (e.g., elliptical-hole PCF) will be difficult to fabricate. The proposed super-lattice structure PCFs concept in this paper indicates a method to achieve PCFs with complex air hole structure which has the potential to overcome the problem that arises during fabrication.

ACKNOWLEDGMENT

This work is supported by the Central Research Grant of The Hong Kong Polytechnic University under the Postdoctoral Fellowship (Project No. G-YX2D).

REFERENCES

1. Birks, T. A., J. C. Knight, and P. S. J. Russel, "Endlessly single-mode photonic crystal fiber," *Opt. Lett.*, Vol. 22, 961–963, 1997.
2. Knight, J. C. and P. S. J. Russell, "Photonic crystal fibers: New way to guide light," *Science*, Vol. 296, 276–277, 2002.
3. Knight, J. C., "Photonic crystal fibers," *Nature*, Vol. 424, 847–851, 2003.
4. Ortigosa-Blanch, A., J. C. Knight, W. J. Wadsworth, J. Arriaga, B. J. Mangan, T. A. Birks, and P. S. J. Russel, "Highly birefringent photonic crystal fibers," *Opt. Lett.*, Vol. 25, 1325–1327, 2000.
5. Ferrando, A., E. Silvestre, J. J. Miret, and P. Andres, "Nearly zero ultraflattened dispersion in photonic crystal fibers," *Opt. Lett.*, Vol. 25, 790–792, 2000.
6. Knight, J. C. and D. V. Skryabin, "Nonlinear waveguide optics and photonic crystal fibers," *Opt. Express*, Vol. 15, 15365–15376, 2007.
7. Fevrier, S., P. Viale, F. Gerome, P. Leproux, P. Roy, J.-M. Blondy, B. Dussardier, and G. Monnom, "Very large effective area singlemode photonic bandgap fibre," *Electron. Lett.*, Vol. 39, 1240–1242, 2003.

8. Dobb, H., K. Kalli, and D. J. Webb, "Temperature-insensitive long period grating sensors in photonic crystal fibre," *Electron. Lett.*, Vol. 40, 657–658, 2004.
9. Dong, X. and H. Y. Tam, "Temperature-insensitive strain sensor with polarization-maintaining photonic crystal fiber based on Sagnac interferometer," *Appl. Phys. Lett.*, Vol. 90, 151113, 2007.
10. Wadsworth, W. J., J. C. Knight, W. H. Reewes, P. S. J. Russell, and J. Arriaga, "Yb³⁺-doped photonic crystal fibre laser," *Electron. Lett.*, Vol. 36, 1452–1253, 2000.
11. Liu, X., X. Zhou, X. Tang, J. Ng, J. Hao, T. Chai, E. Leong, and C. Lu, "Swiathable and tunable multiwavelength erbium-doped fiber laser with fiber Bragg grating and photonic crystal fiber," *IEEE Photon. Technol. Lett.*, Vol. 17, 1626–1628, 2005.
12. Chen, D., "Stable multi-wavelength erbium-doped fiber laser based on photonic crystal fiber Sagnac loop filter," *Laser Phys. Lett.*, Vol. 4, 437–439, 2007.
13. Broderick, N. G. R., T. M. Monro, P. J. Bennett, and D. J. Richardson, "Nonlinearity in holey optical fibers: Measurement and future opportunities," *Opt. Lett.*, Vol. 24, 1395–1397, 1999.
14. Dudley, J. M. and J. R. Taylor, "Ten years of nonlinear optics in photonic crystal fibre," *Nature Photonics*, Vol. 3, 85–90, 2009.
15. Saitoh, K. and M. Koshiba, "Single-polarization single-mode photonic crystal fibers," *IEEE Photon. Technol. Lett.*, Vol. 15, 1384–1386, 2003.
16. Ju, J., W. Jin, and M. S. Demokan, "Design of single-polarization single-mode photonic crystal fiber at 1.30 μm and 1.55 μm ," *J. Lightw. Technol.*, Vol. 24, 825–830, 2006.
17. Chen, D. and L. Shen, "Highly birefringent elliptical-hole photonic crystal fibers with double defect," *J. Lightw. Technol.*, Vol. 25, 2700–2705, 2007.
18. Hu, D. J. J., P. Shum, C. Lu, X. Yu, G. Wang, and G. Ren, "Holey fiber design for single-polarization single-mode guidance," *Appl. Opt.*, Vol. 48, 4038–4043, 2009.
19. Saitoh, K., M. Koshiba, T. Hasegawa, and E. Sasaoka, "Chromatic dispersion control in photonic crystal fibers: Application to ultra-flattened dispersion," *Opt. Express*, Vol. 11, 843–852, 2003.
20. Poletti, F., V. Finazzi, T. M. Monro, N. G. R. Broderick, V. Tse, and D. J. Richardson, "Inverse design and fabrication tolerances of ultra-flattened dispersion holey fibers," *Opt. Express*, Vol. 13, 3728–3736, 2005.

21. Steel, M. J. and R. M. Osgood, "Elliptical-hole photonic crystal fibers," *Opt. Lett.*, Vol. 26, 229–231, 2001.
22. Chen, D. and L. Shen, "Ultrahigh birefringent photonic crystal fiber with ultralow confinement loss," *IEEE Photon. Technol. Lett.*, Vol. 19, 185–187, 2007.
23. Suzuki, K., H. Kubota, S. Kawanishi, M. Tanaka, and M. Fujita, "Optical properties of a low-loss polarization-maintaining photonic crystal fiber," *Opt. Express*, Vol. 9, 676–680, 2001.
24. Wu, J.-J., D. Chen, K.-L. Liao, T.-J. Yang, and W. L. Ouyang, "The optical properties of Bragg fiber with a fiber core of 2-dimension elliptical-hole photonic crystal structure," *Progress In Electromagnetics Research Letters*, Vol. 10, 87–95, 2009.
25. Wang, Z., G. Ren, S. Lou, and S. Jian, "Supercell lattice method for photonic crystal fibers," *Opt. Express*, Vol. 11, 980–991, 2003.
26. Saitoh, K. and M. Koshiba, "Full-vectorial imaginary-distance beam propagation method based on finite element scheme: Application to photonic crystal fibers," *IEEE J. Quantum Electron.*, Vol. 38, 927–933, 2002.
27. Yang, R., W. Xue, T. Huang, and G. Zhou, "Research on the effects of air hole shape on the properties of microstructured optical fibers," *Optical Engineering*, Vol. 43, 2701–2706, 2004.